Kavlicoglu, B. M., Gordaninejad, F., Saiidi, M., and Jiang, Y., "Analysis and Testing of Graphite/Epoxy Concrete Bridge Girders under Static Loading," *Proceedings of Conference on Retrofit and Repair of Bridges*, London, England, July 2001.

ANALYSIS AND TESTING OF GRAPHITE/EPOXY CONCRETE BRIDGE GIRDERS UNDER STATIC LOADING

B. M. Kavlicoglu
Graduate Research Assistant
Mechanical Engineering Department
University of Nevada, Reno, NV 89557, USA

Prof. F. Gordaninejad, Prof. M. Saiidi, & Prof. Y.Jiang
University of Nevada
Reno, NV 89557, USA

KEYWORDS: ANALYSIS, BRIDGE GIRDERS, COMPOSITES, CONCRETE, GRAPHITE/EPOXY, STATIC LOADING

ABSTRACT

An innovative graphite/epoxy–concrete (G/E-C) cross-section was developed and tested under two-point static loading. Finite element analysis and theoretical modeling of the cross-section was performed. The cross-section was a box girder with an outer G/E U-beam and inner G/E box beam with concrete webs and flange in between. Shear connection between G/E box beam and concrete slab was provided by a two-part structural epoxy resin. Additional shear connection was provided by steel stirrups located at 254 mm (10 in.) spacing along longitudinal axis of the test specimen. It was observed that, steel stirrups contributed the load carrying capacity after initiation of slippage between G/E beams and concrete. Moreover, a series of bond strength tests were performed to examine the behavior of structural epoxy resin for connection between G/E and concrete. Six G/E strips were subjected to tensile tests to evaluate the longitudinal and transverse elastic moduli of the laminate. Using the proper material properties and assumptions, it was possible to demonstrate the behavior of the section under static loads theoretically and in finite element analysis.

INTRODUCTION

In recent years, advanced composite materials in the form of fiber reinforced plastics (FRP's) have found application in infrastructures, mainly in bridges in the form of deck reinforcement and retrofit of columns. The basic reasons behind this development are increasing deficiency rates of current infrastructure and many advantages of composite materials over conventional infrastructure materials such as steel. Since the advantages of composite materials were well defined by aerospace industry, it has been thought that composites should overcome the problems in infrastructure.

The United States Federal Highway Administration reported that 31.4 % of United States' 582,000 bridges were structurally deficient or needed repair (Anido et al. 1998). It was also reported that the bridges constructed in 1960's and 1970's were designed to last for 40-50 years. Therefore, in the near future most of the bridges in the US will need major repair and strengthening. The deficiencies were mainly due to environmental effects (corrosion, fire, earthquake etc.), increased social needs such as traffic loads, changing design codes and increase in safety features. The cost to repair or retrofit all deficient bridges is estimated to be around $50 billion, although only $5 billion is available in the budget for this purpose (Hayes 1998). Not only the US, but also Japan and most of the countries in Europe are suffering from the same problem. Therefore, in the last two decades scientists and researchers have been searching for new design concepts for a more durable and more cost effective bridges. Composite materials have been extensively used in aerospace applications and their properties are well known. Therefore in the search for new design concepts and repair solutions FRP`s offer a strong solution with their superior properties.

This paper presents a summary of the experimental and analytical study of the static behavior of a new graphite/epoxy-concrete beam type.

DEVELOPMENT OF A NEW GIRDER DESIGN

Conventional composite bridge construction makes use of steel girders and reinforced concrete bridge slabs that are connected to the steel girder by shear studs. A new girder was developed in this study in which the steel girder is replaced by a graphite composite/concrete (G/E/C) box beam. The horizontal shear is transferred to between the beam and the slab by a series of steel stirrups. Details of the new beam are presented in the description of the beam specimen in the following sections. The experimental and analytical studies described in this paper were undertaken to evaluate the response of the proposed girder and identify areas of needed improvement.

A quarter scale beam specimen was constructed and tested under two-point static loading. The main goals were to observe the overall behavior of the cross-section and to evaluate the shear connection performance in transferring stresses between the G/E/C beam and concrete slab.

Test Specimen

The dimensions of the cross-section of the specimen can be seen in Fig.1. The outer shell of this box girder was composed of a 230 mm wide x 205 mm deep x 8 mm thick (9-1/16 in. wide x 8-1/16 in. deep x 5/16 in. thick) graphite/epoxy channel section. The inner section was 157 mm wide x 157 mm deep x 8 mm thick (6-3/16 in. wide x 6-3/16 in. deep x 5/16 in. thick) graphite/epoxy box. Each composite beam had a stacking sequence of 42-layer symmetric angle ply laminate ($[90°/(+7°/-7°)_3]_{6s}$) (Jones 1999). The graphite/epoxy elements were manufactured by filament winding method. The space in between the channel and box elements was filled with concrete. The concrete layer thickness was 28.5 mm (1-1/18 in.) at the webs and 30 mm (1-3/16 in.) thick at the bottom flange. The concrete slab had a thickness of 60 mm (2-3/8 in.) and a width of 710 mm (28 in.). The upper 13 mm (½ in.) of the channel beam was embedded in the bottom of concrete. The concrete used in the specimen was normal weight concrete with a maximum aggregate size of 10 mm (3/8 in.). The target concrete compressive strength was 41 MPa (6,000 psi).

Slab of the beam was reinforced by #3 (ϕ 10 mm) steel bars according to ACI 318-95 (ACI 1989) minimum shrinkage steel requirement. Shear connection between the G/E/C beam and the slab was provided through an epoxy resin and steel stirrups. It was estimated that at a certain load limit the epoxy bond connecting would fail and the forces would transfer to the stirrups. For this purpose, #3 (ϕ 10 mm) stirrups were placed around G/E box beam at a center-to-center spacing of 254 mm (10 in.). These stirrups were tied to two #3 (ϕ 10 mm) longitudinal steel bars in the slab (Fig. 2).

The girder prior to the placement of concrete is shown in Fig. 2. To facilitate concrete placement in the bottom flange and the webs of the G/E/C beam, ASTM C494 Type-F Daracem superplasticizer was used to improve the workability of the concrete. Before pouring the first batch, top flanges of the box beams were covered with a protective sheet to keep them clean, because epoxy adhesive was going to be applied to top flanges of the box beams. While second batch was being mixed, LORD 304 (Lord Corporation) two-part epoxy adhesive was also mixed with 2:1 resin: hardener ratio. After the epoxy was applied to the top flange of the box beam, the second batch of concrete was poured in the slab and was vibrated.

Instrumentation and Testing

The cross-section developed in this study was equipped with single strain gages, strain gage rosettes, Novotechnik displacement transducers, and Temposonic displacement transducers in order to capture the behavior of the cross-section under the applied load. Vishay CEA-13-125UN-350 strain gages and Vishay CEA-13-125UR-350 rosettes were used at various critical locations of the beams. Strain gages were installed on stirrups at constant moment sections. At mid span, a total of 6 strain gages were installed on the top flange of box beam, lower flange of channel beam and lower flange of the box beam. Rosettes were installed on webs of channel beam and box beam. The Novotechnik transducers were

used to determine the strain profile at mid span and measure slippage between the concrete slab and the G/E/C beam at the supports. Two Novotechnik transducers with an allowable stroke of ± 50.8 mm (± 2 in.) were installed to the top and bottom flanges of the concrete slab at mid span. Additionally, two Novotechnik transducers with an allowable stroke of ± 152.4 mm (± 6 in.) were installed on the web of the graphite/epoxy channel beam. Two other 50.8 mm (± 2 in.) stroke Novotechnik transducers were installed at ends of the specimens and were used to measure slippage. Two Temposonic transducers with an allowable stroke of 910 mm (36 in.) were attached to the corners of flange of the channel beam at mid span of the girder. These transducers were used to measure the vertical deflection of the beam and to determine possible twisting of the girder.

The testing of the specimen was load controlled initially. Load was applied at 22.2 kN (5 kips) increments. At the end of each loading step, loading was stopped and specimen was visually inspected for concrete cracks, delamination of graphite/epoxy sections, etc. Load controlled testing was performed until the stiffness began to reduce due to cracking and slippage. After this point loading was displacement controlled. Loading of the specimen continued until the failure of the structure occurred.

In addition to the beam test, coupon tests to determine the composite material properties and bond strength test to assess the shear transfer between concrete and G/E plates connected by epoxy were conducted the details of which can be found in Kavlicoglu (2000).

Test Results

The force vs. displacement curve for static girder test is shown in Fig. 3. Initiation of slippage between graphite/epoxy channel beam and concrete was observed at a load of 81.4 kN (18.3 kips). The small drop in the load indicated the start of slippage. As loading continued, the channel element continued to debond from the concrete slab. Major slippage between the box beam and concrete slab and the corresponding visible reduction in the stiffness occurred at a load of 214 kN (48.1 kips). This load was the load at which epoxy bond failure initiated at the left end of the girder. After this load, the channel beam continued to debond and the top of its webs separated from the concrete slab over one-third of the length of the beam from each end. Local bearing damage of channel element and cracking of the concrete in the web of the G/E/C beam were also observed at the supports. The concrete in the support zones was strengthened by an epoxy mortar. Meanwhile, flange of the channel beam delaminated at the very ends of the beam. Another major slippage occurred at a load of 260 kN (58.4 kips). This debonding was followed by gradual debonding of box and channel beam until failure point was reached at 376.3 kN (84.6 kips) and at a deflection of 48.3 mm (1.9 in). The failure mode was the shear of the graphite/epoxy box beam. Figure 4 shows the web shear cracks in the concrete after the removal of the channel section. The shear failure extended into the G/E box element.

Since there was no physical connection between channel beam and concrete, debonding began even at low load values. As debonding continued, webs of the channel beam lost their load carrying capacity. At the end of the experiment, it was observed that, a 508 mm (20 in) portion of the webs in the middle of the girder was still bonded to the slab.

The strain values for stirrups showed a sudden increase when initial bond slippage at 214 kN (48.1 kips) occurred. This indicated the effectiveness of the stirrups to resist the horizontal shear. Maximum strain recorded on the stirrups at failure of the girder was 1527 microstrain, which was 66.4% of yield strain for steel.

Normal strain data for G/E elements showed that the stress-strain behavior was linear both in tension and compression, and also the slopes of force vs. strain curves were very close, which implies that, effective modulus of elasticity was same in compression and tension. The normal strains increased at a much higher rate upon the initial debonding at the load of 214 kN (48.1 kips) as can be seen in Fig. 5.

The tensile strain on the lower flange of box beam just before failure was 4927 microstrain, while it was 1812 microstrain on lower flange of channel element, further confirming that the slippage had taken place between the channel section and concrete. These results showed that the contribution of the channel section was limited due to debonding. The ultimate compressive strain was 4483 microstrain in the upper flange of box element.

The vertical deflections at the two edges of the slab at mid span of the girder were nearly identical. This meant that there was no twisting action of the beam.

The vertical force versus horizontal slippage relationship at the ends of the girder showed trends that were consistent with the measured load-deflection diagram of the girder. At a load of 241 kN (48.1 kips), the slippage was close to 4 mm (0.16 in.). At the ultimate load, slippage value for the west end was 5.39 mm (0.21 in), while it was 2.97 mm (0.12 in) at the east end.

FINITE ELEMENT ANALYSIS

Finite element analysis of the girder was conducted both prior to finalizing the design and after the tests. The pretest analyses helped in the refinement of the design to ensure that high horizontal shear stresses would be developed at the interface between the concrete slab and the remainder of the girder. The analyses after the tests helped explain the behavior of the girder.

ANSYS 5.5 software was used for finite element modeling. To reduce the number of elements and node numbers, symmetry of the beam was used and only a quarter of the girder was modeled with appropriate boundary conditions. The following assumptions were made in the finite element model:

- Model included both material (concrete, steel) and geometric nonlinearity.
- Perfect bond among elements was assumed, i.e. there was no slippage in the model.
- The stress-strain relationship of concrete elements was modeled according to the Hognestad model.
- Shrinkage reinforcements in the slab were not included in the model.
- Graphite/epoxy elements were modeled as a single layer orthotropic material using equivalent material properties.
- Tensile and compressive behavior of graphite/epoxy was assumed to be same.
- Non-uniformity of graphite/epoxy elements was neglected.
- Steel stirrups were modeled as brick elements.

Finite Element Model

The one-quarter finite element consisted of 2975, 8-noded brick elements and 3928 nodes. SOLID 65 element type was used for concrete and composite, and SOLID 45 element type was used for steel elements. Table 1 summarizes the element types and material properties used in ANSYS 5.5. Nonlinear stress-strain curves of concrete and steel were incorporated in the model using ANSYS' "Multi-linear Kinematic Hardening" option. The real stress-strain curves were approximated by a series of straight lines. Finer meshes were generated at load and support areas to provide a more uniform loading condition.

The one-quarter model was developed as a cantilever beam with mid span of the girder modeled as the fixed end (Fig. 6). At this end, all degrees of freedom were restrained. The applied loads on the girder and the reactions (Equal to the applied load on the quarter model) were applied as external loads on the finite element model.

Finite Element Analysis Results

As mentioned earlier, during the girder testing the upper part of G/E channel element separated from concrete and the webs of channel beam did not contribute to the load carrying capacity. To capture the

behavior of the girder a range of contribution of the channel element was considered. Three different finite element models were developed using assuming different percentages of channel web elements being present. At the end of testing of specimen, it was observed that there was a 0.66-m (26-in.) portion of the channel beam still in contact with concrete, which corresponds to 30% of the channel length. To model the loss of contacted areas, stiffness of the debonded graphite/epoxy elements was reduced by a factor of 1000, instead of removal of those elements to prevent the continuity in the finite element model. The stiffness of the remaining 30% of the channel web elements was held constant. Similarly, another analysis was conducted by reducing the stiffness of all the elements in channel element webs (0% channel web elements). The force-displacement curves obtained from these 3 models were superimposed on the experimental data in Fig. 7. It can be observed that, in the absence of slippage, finite element model works led to a near perfect match with the experimental data. After the initiation of slippage and stiffness reduction, slope of experimental data, became close to the slope of FE result with 30% web being effective. Finally when the webs of the channel section were completely removed, the calculated stiffness was considerably below the measured value. The FE analysis results demonstrated that the upper and lower bound of the actual behavior can be captured with reasonable accuracy.

SIMPLIFIED ANALYSIS

A simple linear analysis was performed to estimate the theoretical mid-plane deflection of the beam under static loading. Such as analysis would be of the type conducted by a design engineer. Equivalent elastic modulus and equivalent moment of inertia calculations were based on transformed cross section method presented in (Wang et al. 1985). For the transformed cross-section graphite/epoxy materials were transformed into equivalent area of concrete. This transformation was based on the modular ratio, which was equal to the ratio of modulus of elasticity of G/E over the modulus of elasticity of concrete.

The theoretical and experimental load-deflection curves are shown in Fig. 8. The simple model predicted the initial stiffness of the beam closely. However, after the non-linearity of concrete and initiation of slippage affected the behavior at a load of 214 kN (48.1 kips), the experimental curve deviated from the theoretical one due to the reduction in stiffness, and theoretical curve overestimated the stiffness.

CONCLUSIONS

In this study, it was demonstrated that, the use of steel stirrups as shear connection elements for composite/concrete bridge girders worked effectively. Initiation of slippage in epoxy bonded areas indicated the reduction in stiffness and transfer of horizontal shear to the stirrups. However, after the bond failure steel stirrups contributed to the load carrying capacity. Finite element analysis and a simple theoretical analysis showed that, using proper assumptions, it was possible to model the behavior of the new graphite/epoxy/concrete girder.

REFERENCES

ACI (American Concrete Institute), *"Building Code Requirements for Reinforced Concrete (ACI 318-95),"* Detroit, MI, 1995.

Anido, R.L., Troutman, D.L., Busel, J.P., "Fabrication and Installation of Modular FRP Composite Bridge Deck," *Proceedings of the 1998 International Composites Expo*, Nashville, Tennessee, January 19-21, 1998, Session 4-A, pp. 1-6.

Kavlicoglu, B., "Enforcement of Shear Connection in FRP/Concrete Bridge Girders," A thesis submitted in partial fulfillment of the degree of MSME, University of Nevada, Reno, August 2000.

Hayes, M.D., "Characterization and Modeling of a Fiber-Reinforced Polymeric Composite Structural Beam and Bridge Structure for Use in the Tom`s Creek Bridge Rehabilitation Project," *M.S. Thesis in Engineering Mechanics*, Virginia Polytechnic Institute and State University, Blacsburg, Virginia, 1998.

LORD Corporation Chemical Products Division, 18203 Mt. Baldy Circle, Fountain Valley, CA 92708, http://www.lordcorporation.com .

Kavlicoglu, B. M., Gordaninejad, F., Saiidi, M., and Jiang, Y., "Analysis and Testing of Graphite/Epoxy Concrete Bridge Girders under Static Loading," *Proceedings of Conference on Retrofit and Repair of Bridges*, London, England, July 2001.

Wang, C., Salmon, C.G., "*Reinforced Concrete Design*," 4th edition, Harper & Row Publishers, New York, NY, 1985.

ACKNOWLEDGEMENTS

The study presented in this article was funded by Grant CMS-9800080 from the US National Science Foundation. The support of the NSF program director for the project, Dr. Jack Scalzi, is appreciated.

Table 1. Element Types and Material Properties used in ANSYS 5.5

Element # (1)	ANSYS Element Type (2)	Element (3)	Material Properties (4)
1	SOLID65	Concrete in compression	E_c= 30.2 GPa ν_c= 0.15
2	SOLID45	Graphite/epoxy	E_{11}= 95,150 MPa E_{22}= 11,639 MPa ν_{12}= 0.3 G_{12}= 6,520 MPa
3	SOLID45	Steel	E_s= 200 Gpa ν_s= 0.3
4	SOLID65	Concrete in tension	E_c= 30.2 GPa ν_c= 0.15

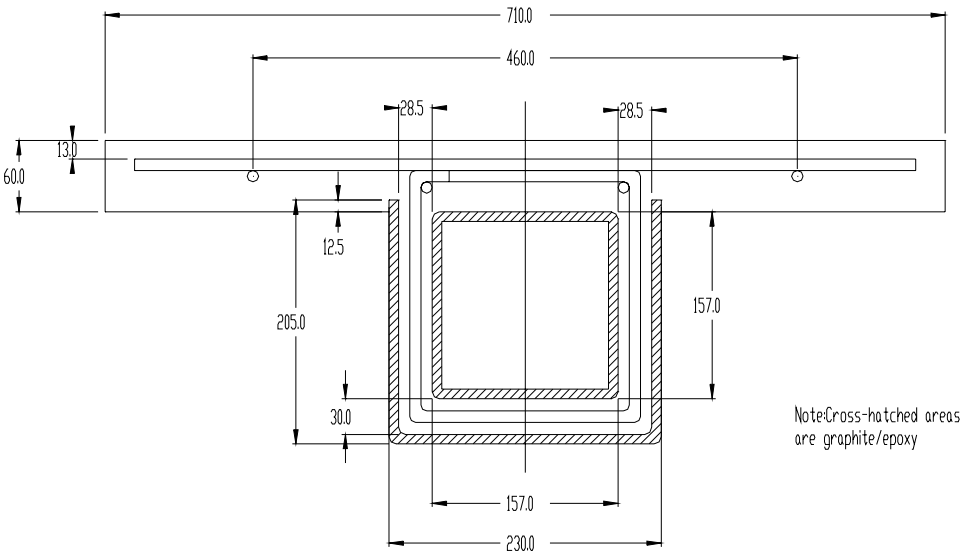

Fig. 1 Cross Section of the New G/E/C Girder

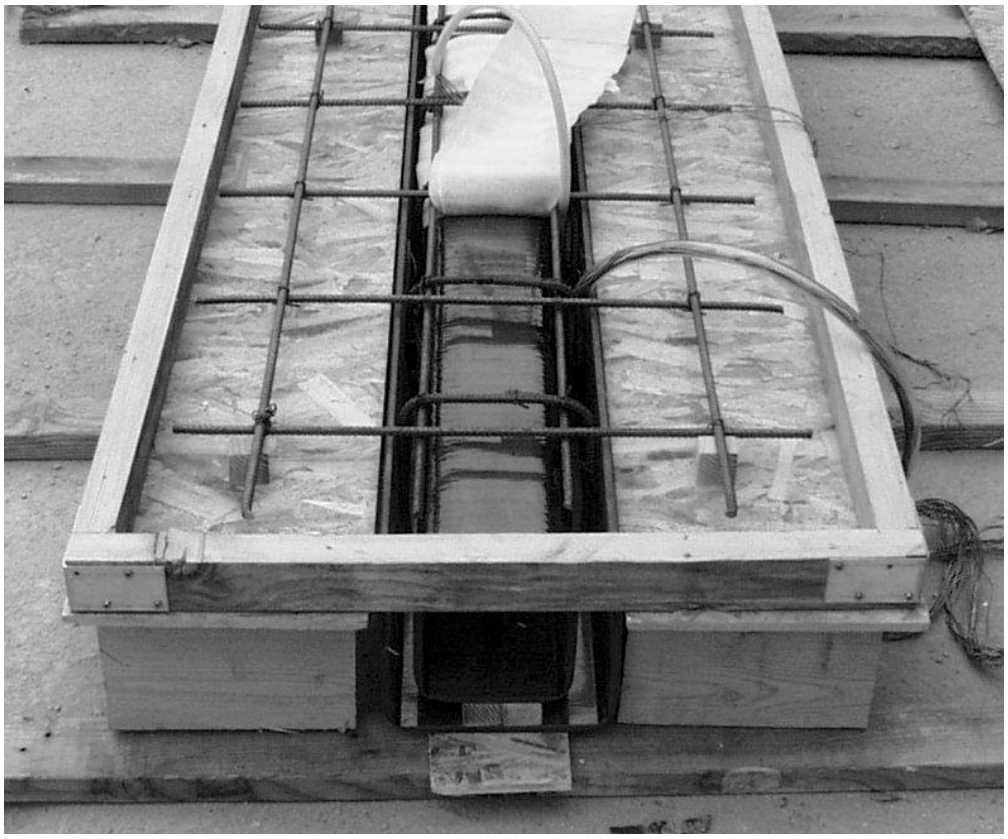

Fig. 2 New Girder Before Concrete Placement

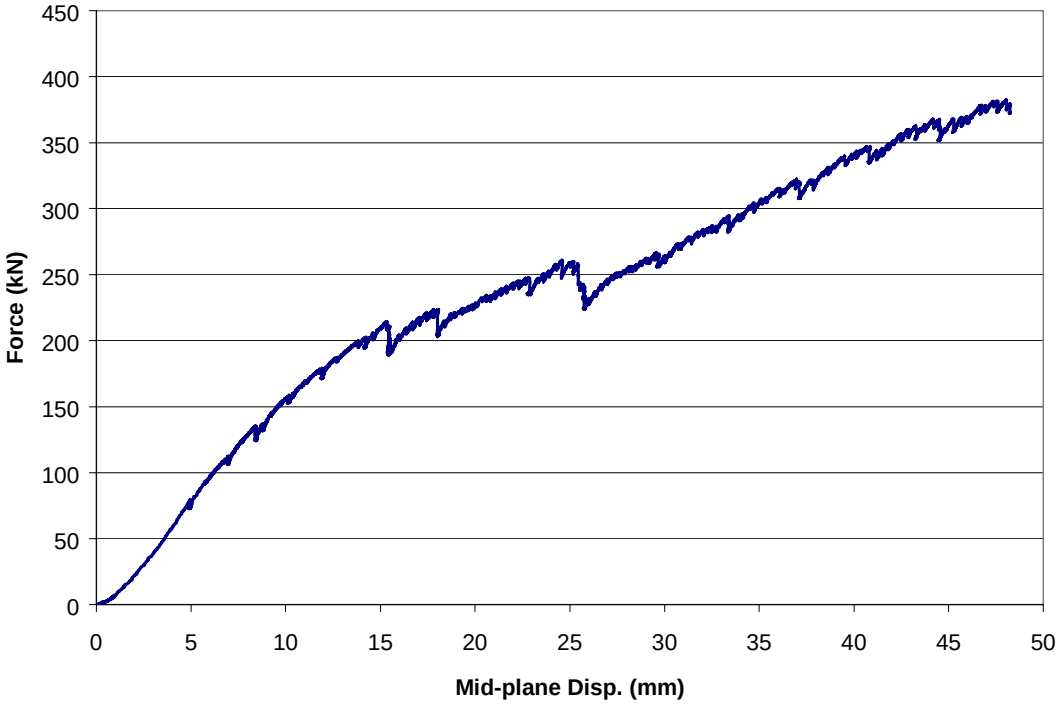

Fig. 3 Force vs. Mid-Plane Displacement Curve for Static Test

Fig. 4 Shear Crack Pattern in Concrete Web

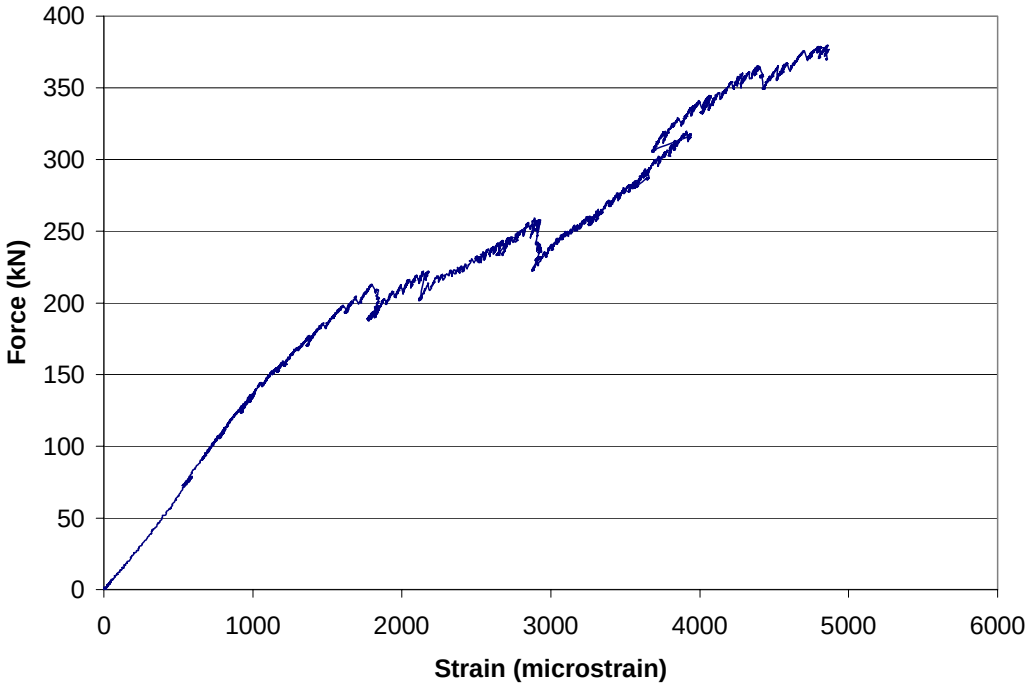

Fig. 5 Strain Data for Bottom Flange of the G/E Box Element

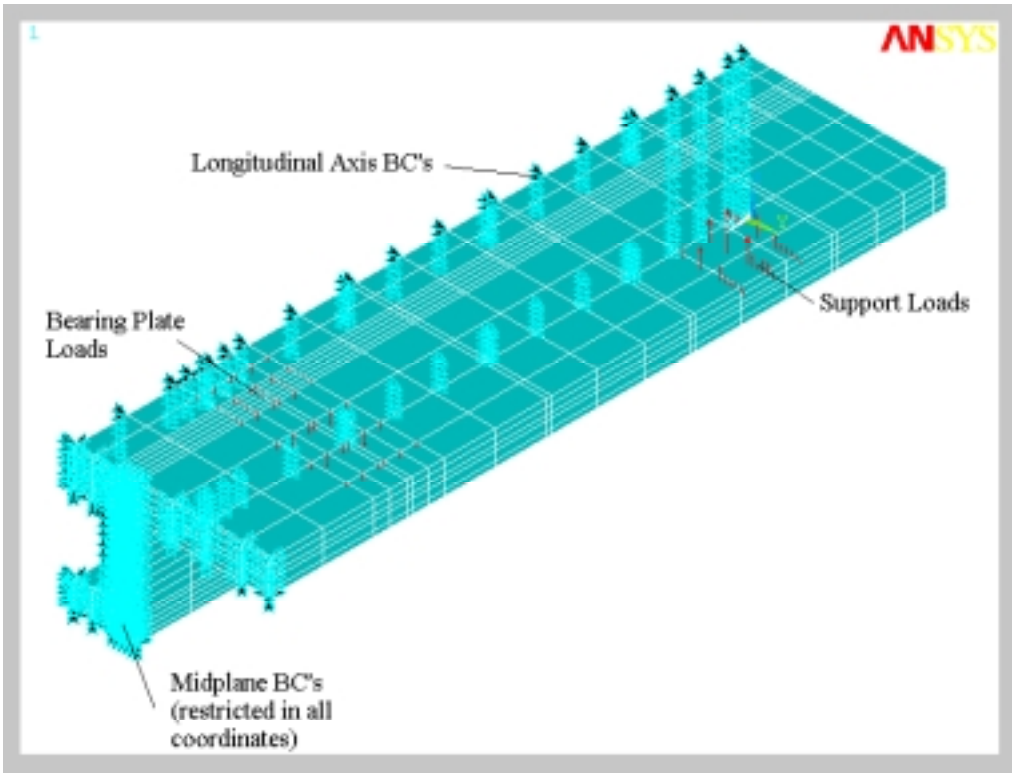

Fig. 6 One-quarter FEA Model Developed in ANSYS 5.5

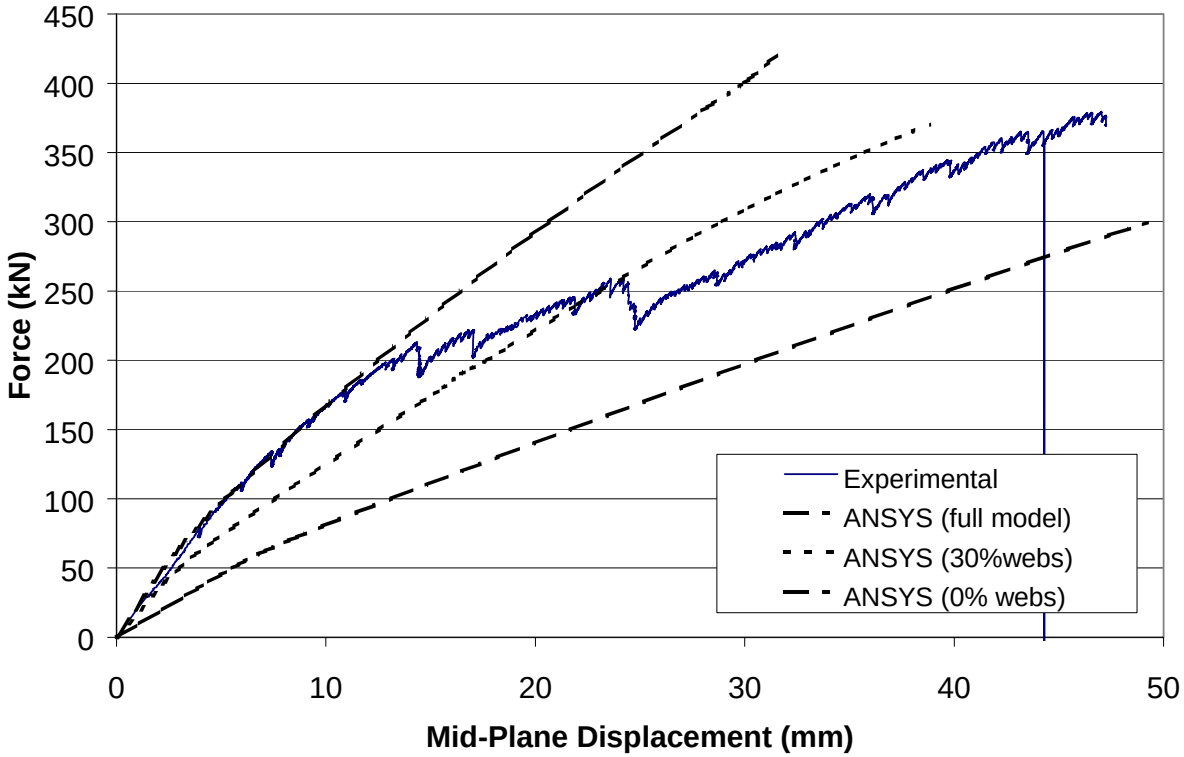

Fig. 7 Comparison of Experimental and FEA Results

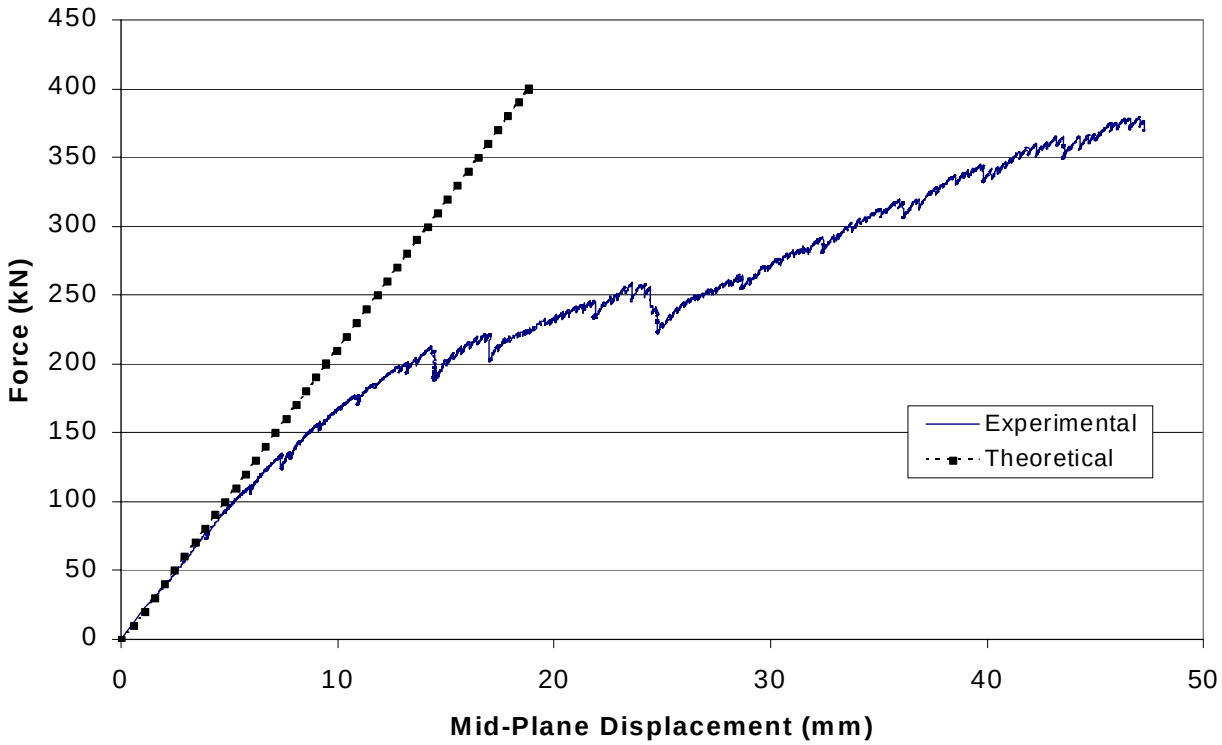

Fig. 8 Comparison of Simplified Theoretical and Experimental Results